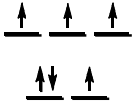
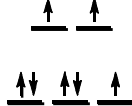
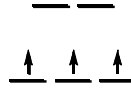
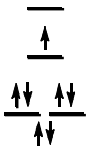
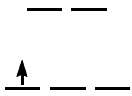
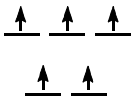
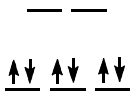
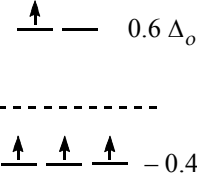
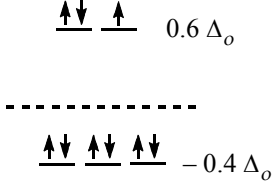
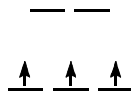
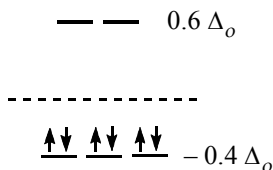


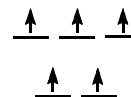
CHAPTER 10: COORDINATION CHEMISTRY II: BONDING

- 10.1 a. Tetrahedral d^6 , 4 unpaired electrons 
- b. $[\text{Co}(\text{H}_2\text{O})_6]^{2+}$, high spin octahedral d^7 , 3 unpaired electrons 
- c. $[\text{Cr}(\text{H}_2\text{O})_6]^{3+}$, octahedral d^3 , 3 unpaired electrons 
- d. square planar d^7 , 1 unpaired electron 
- e. $5.1 \text{ BM} = \mu = \sqrt{n(n+2)}$; $n = 4.2 \approx 4$
- 10.2 a. $[\text{M}(\text{H}_2\text{O})_6]^{3+}$ with 1 unpaired electron. d^1 :  $\text{M} = \text{Ti}$
- b. $[\text{MBr}_4]^-$ with the maximum number of unpaired electrons (5). 
 M^{3+} with 5 d electrons: $\text{M} = \text{Fe}$
- c. Diamagnetic $[\text{M}(\text{CN})_6]^{3-}$. The strong field cyano ligand favors low spin. M^{3+} with 6 d electrons: $\text{M} = \text{Co}$ 
- d. $[\text{M}(\text{H}_2\text{O})_6]^{2+}$ having $\text{LFSE} = -\frac{3}{5}\Delta_o$. Both high spin d^4 and d^9 have the correct Δ_o .
- High spin d^4 : $\text{M} = \text{Cr}$  $0.6 \Delta_o$ $-0.4 \Delta_o$
- d^9 : $\text{M} = \text{Cu}$  $0.6 \Delta_o$ $-0.4 \Delta_o$
- 10.3 a. $\text{K}_3[\text{M}(\text{CN})_6]$ M is first row transition metal, 3 unpaired electrons. 
 M^{3+} with 3 d electrons: $\text{M} = \text{Cr}$

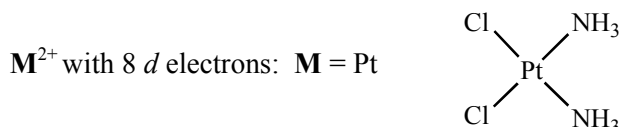
- b. $[\text{M}(\text{H}_2\text{O})_6]^{3+}$ **M** is second row transition metal, $\text{LFSE} = -2.4 \Delta_o$. This can be achieved with a low spin d^6 configuration. M^{3+} with 6 d electrons: **M** = Rh



- c. $[\text{MCl}_4]^-$ **M** is first row transition metal, 5 unpaired electrons. M^{3+} with 5 d electrons: Fe



- d. $\text{MCl}_2(\text{NH}_3)_2$ **M** is third row d^8 transition metal; two **M**–Cl stretching bands in IR. Second and third row d^8 complexes are often square planar. The presence of two **M**–Cl stretching bands implies *cis* geometry of the chloro ligands.



10.4 Angular overlap calculations for d^8 and d^9 ions show no energy difference between D_{4h} and O_h when exclusively considering σ interactions. Both d^8 geometries have energies of $-3e_\sigma$; both d^9 geometries have energies of $-6e_\sigma$. In general, stability constants decrease as more ligands are added; the sequence for nickel is the common one. The huge drop in stability constant between the second and third ethylenediamine on Cu^{2+} is a result of the d^9 Jahn-Teller effect. The first two en ligands add in a square-planar geometry, with water molecules in the axial positions, and the coordination of these two monodentate ligands allows for the Jahn-Teller distortion. Adding a third en ligand requires a geometry change and with a preference for uniform **M**–**N** bond distances towards the six nitrogen atoms. This is counter to the Jahn-Teller distortion, and the third addition is much less favorable than the first two.

- 10.5** $[\text{M}(\text{H}_2\text{O})_6]^{2+}$ **M** is first row transition metal, $\mu = 3.9 \text{ BM}$. The magnetic moment implies 3 unpaired electrons, which would give rise to $\mu = \sqrt{3(3+5)} = 3.9 \text{ BM}$. There are two possibilities, d^3 and d^7 :



- 10.6**
- a. $[\text{Cr}(\text{H}_2\text{O})_6]^{2+}$ $n = 4$
 $\mu = \sqrt{4(6)} = 4.9 \mu_B$
- b. $[\text{Cr}(\text{CN})_6]^{4-}$ $n = 2$
 $\mu = \sqrt{2(4)} = 2.8 \mu_B$
- c. $[\text{FeCl}_4]^-$ $n = 5$
 $\mu = \sqrt{5(7)} = 5.9 \mu_B$
- d. $[\text{Fe}(\text{CN})_6]^{3-}$ $n = 1$
- e. $[\text{Ni}(\text{H}_2\text{O})_6]^{2+}$ $n = 2$
 $\mu = \sqrt{2(4)} = 2.8 \mu_B$
- f. $[\text{Cu}(\text{en})_2(\text{H}_2\text{O})_2]^{2+}$ $n = 1$
 $\mu = \sqrt{1(3)} = 1.7 \mu_B$

- 10.7** $\text{Fe}(\text{H}_2\text{O})_4(\text{CN})_2$ is really $[\text{Fe}(\text{H}_2\text{O})_6]_2[\text{Fe}(\text{CN})_6]$, all containing Fe(II). $[\text{Fe}(\text{H}_2\text{O})_6]^{2+}$ is high spin d^6 , with $\mu = 4.9 \mu_B$; $[\text{Fe}(\text{CN})_6]^{4-}$ is low spin d^6 , with $\mu = 0 \mu_B$. The average value is then $2 \times 4.9/3 = 3.3 \mu_B$.

2.67 unpaired electrons gives $\mu = \sqrt{2.67 \times 4.67} = 3.53 \mu_B$.

- 10.8** Co(II) is d^7 . In tetrahedral complexes, it is generally high spin and has 3 unpaired electrons; in octahedral complexes, it is also typically high spin and also has 3 unpaired electrons; in square planar complexes, it has 1 unpaired electron. The magnetic moments can be calculated as $\mu = \sqrt{n(n+2)} = 3.9, 3.9, \text{ and } 1.7 \mu_B$, respectively.
- 10.9** For the red compounds (Me and Et at high temperatures, Pr, pip, and pyr at all temperatures), the larger magnetic moment indicates approximately 5 unpaired electrons, appropriate for high-spin Fe(III) species. At low temperatures for the Me and Et compounds, the magnetic moment indicates 3 to 4 unpaired electrons, an average value indicating an equilibrium mixture of high and low spin species. The low spin octahedral complexes have 1 unpaired electron. Increasing the size of the R groups changes the structure enough that it is locked into high-spin species at all temperatures.
- 10.10** Both $[\text{M}(\text{H}_2\text{O})_6]^{2+}$ and $[\text{M}(\text{NH}_3)_6]^{2+}$ should show the double-humped curve of Figure 10.12, with larger values for the NH_3 compounds. Therefore, the difference between these curves shows the same general features as in Figure 10.12.
- 10.11** These can be verified using the approach introduced in Chapters 4 and 5, in which a character of +1 is counted for each operation that leaves a vector unchanged, a character of -1 for each operation that leaves a vector in its position, but with the direction reversed. The general transformation matrix for rotation is provided in Figure 4.16. Application of this matrix is necessary to deduce the characters involving rotations.
- 10.12** The e_σ column gives d orbital energies for complexes involving σ donor ligands only; the Total column gives energies for complexes of ligands that act as both σ donors and π acceptors:

- a. ML_2 , using positions 1 and 6:

	e_σ	e_π	Total
z^2	2	0	$2e_\sigma$
x^2-y^2	0	0	0
xy	0	0	0
xz	0	-2	$-2 e_\pi$
yz	0	-2	$-2 e_\pi$

- b. ML_3 , using positions 2, 11, 12:

	e_σ	e_π	Total
z^2	0.75	0	$0.75e_\sigma$
x^2-y^2	1.125	-1.5	$1.125 e_\sigma - 1.5 e_\pi$
xy	1.125	-1.5	$1.125 e_\sigma - 1.5 e_\pi$
xz	0	-1.5	$-1.5 e_\pi$
yz	0	-1.5	$-1.5 e_\pi$

c. ML_5, C_{4v} , using positions 1, 2, 3, 4, 5:

	e_σ	e_π	Total
z^2	2	0	$2e_\sigma$
x^2-y^2	3	0	$3e_\sigma$
xy	0	-4	$-4e_\pi$
xz	0	-3	$-3e_\pi$
yz	0	-3	$-3e_\pi$

d. ML_5, D_{3h} , using positions 1, 2, 6, 11, 12:

	e_σ	e_π	Total
z^2	2.75	0	$2.75e_\sigma$
x^2-y^2	1.125	-1.5	$1.125 e_\sigma - 1.5 e_\pi$
xy	1.125	-1.5	$1.125 e_\sigma - 1.5 e_\pi$
xz	0	-3.5	$-3.5 e_\pi$
yz	0	-3.5	$-3.5 e_\pi$

e. ML_8 , cube, positions 7, 8, 9, 10, doubled for the other four corners:

	e_σ	e_π	Total
z^2	0	-5.33	$-5.33 e_\pi$
x^2-y^2	0	-5.33	$-5.33 e_\pi$
xy	2.67	-1.78	$2.67 e_\sigma - 1.78 e_\pi$
xz	2.67	-1.78	$2.67 e_\sigma - 1.78 e_\pi$
yz	2.67	-1.78	$2.67 e_\sigma - 1.78 e_\pi$

10.13

Metal d orbitals, NH_3 influence

	e_σ	e_π	Total
z^2	1	0	$1e_\sigma$
x^2-y^2	3	0	$3e_\sigma$
xy	0	0	0
xz	0	0	0
yz	0	0	0

Ligand NH_3 :

	e_σ	Total
1	0	0
2	-1	$-1e_\sigma$
3	-1	$-1e_\sigma$
4	-1	$-1e_\sigma$
5	-1	$-1e_\sigma$
6	0	0

Metal d orbitals, Cl^- influence

	e_σ	e_π	Total
z^2	2	0	$2e_\sigma$
x^2-y^2	0	0	0
xy	0	0	0
xz	0	2	$2 e_\pi$
yz	0	2	$2 e_\pi$

Ligand Cl^- :

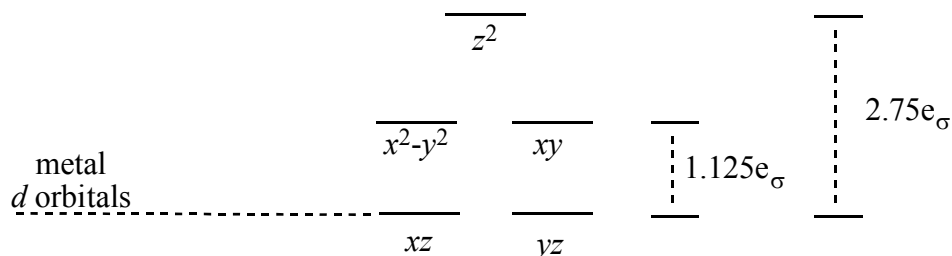
	e_σ	e_π	Total
1	-1	-2	$-1e_\sigma - 2 e_\pi$
2	0	0	0
3	0	0	0
4	0	0	0
5	0	0	0
6	-1	-2	$-1e_\sigma - 2 e_\pi$

Overall energy = $-8 e_\sigma(NH_3) - 4 e_\sigma(Cl) - 8 e_\pi(Cl) + 4 e_\pi(Cl) = -8 e_\sigma(NH_3) - 4 e_\sigma(Cl) - 4 e_\pi(Cl)$

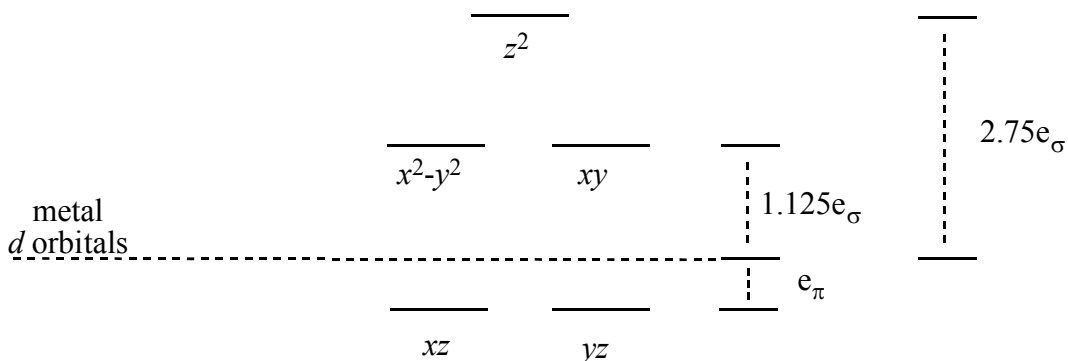
The metal electrons are still unpaired, one in the d_{xy} orbital and one each in the d_{xz} and d_{yz} , raised by π interaction with Cl^- . Four of the ligand orbitals are lowered by $e_\sigma(NH_3)$ and two are lowered

by $e_{\sigma}(\text{Cl}) + 2 e_{\pi}(\text{Cl})$; each contains a pair of ligand electrons. The precise orbital energies cannot be calculated since the angular overlap parameters for NH_3 and Cl towards $\text{Cr}(\text{III})$ are not provided. Table 10.13 does provide the necessary parameters for $\text{trans-}[\text{Cr}(\text{NH}_3)_4\text{F}_2]^+$.

- 10.14 a. If we assume these ligands have similar donor abilities, the energies below are obtained for the molecular orbitals with high d orbital character.

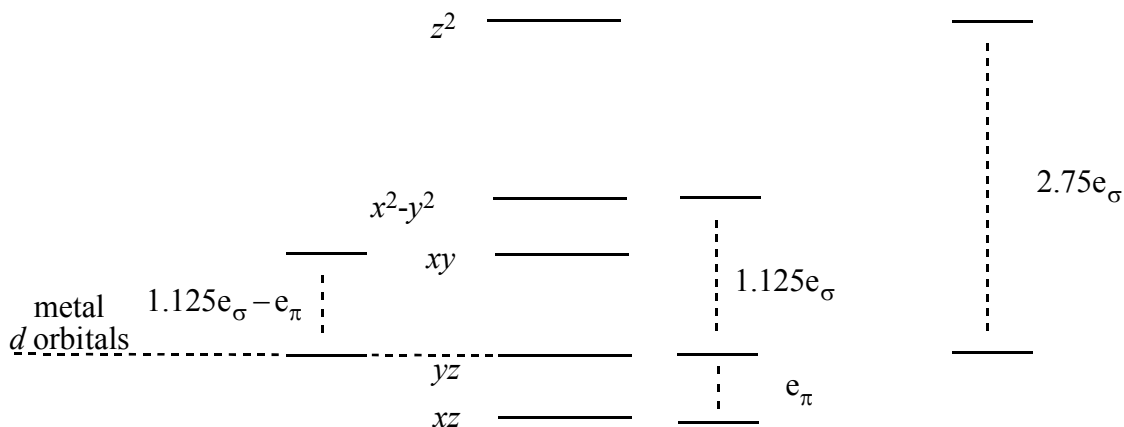


- b. For consideration of L' as a π -acceptor in the axial position, the identical energy level diagram is obtained regardless of whether L' is assigned to position 1 or 6. The xz and yz orbitals are each stabilized by e_{π} .

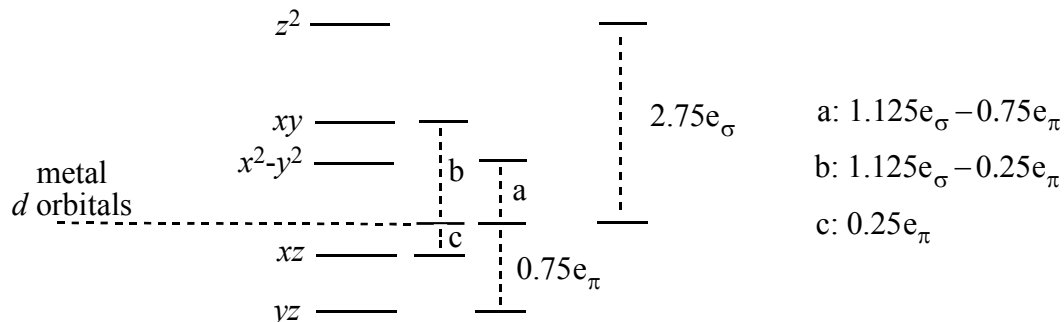


For consideration of L' in an equatorial position, the angular overlap result is different depending on whether the π -acceptor is placed in position 2 or position 11/12. This is problematic since all three equatorial positions are indistinguishable.

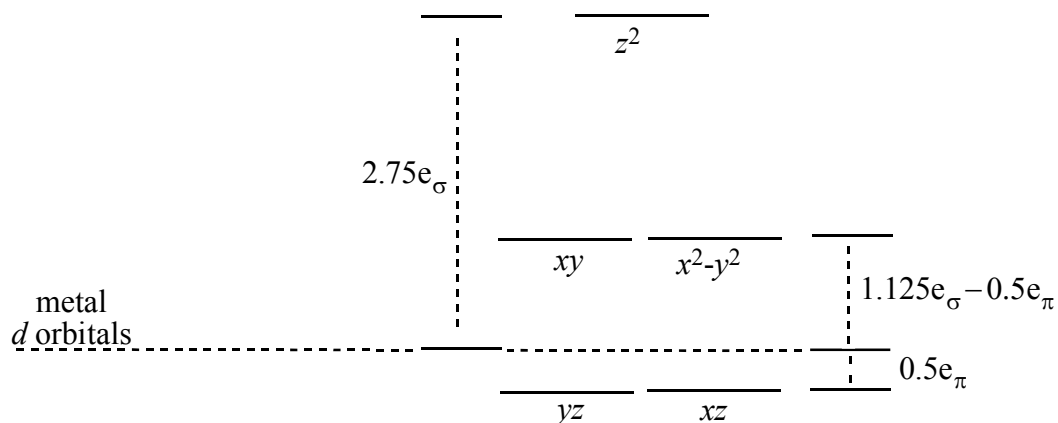
For L' in position 2:



For L' in position 11 or 12:



Since all three equatorial sites are equivalent, the optimum approach is to consider the weighted average of these two equatorial diagrams, with the second one contributing twice as much as the first since the second diagram is obtained with L' in both position 11 and position 12. This average diagram is below:

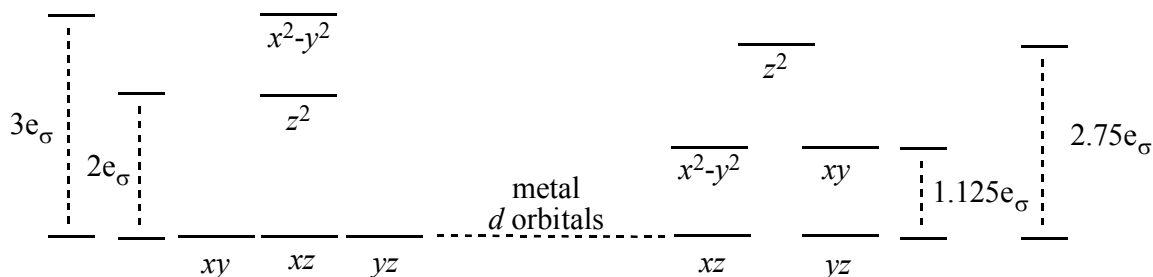


- c. The axial/equatorial preference for the π -acceptor ligand depends on the number of metal valence electrons. The table below assumes low-spin configurations, reasonable on the basis of the π -acceptor ligand. Alternate configuration energies would be obtained for high-spin cases. This analysis predicts that the axial position would be preferred for the π -acceptor ligand in d^1 to d^7 cases. There is no difference between the configuration energies for the d^8 to d^{10} cases. This analysis includes neither the exchange energy nor the coulombic energy of repulsion contributions. Ligand positions are strongly influenced by steric considerations, also not accounted for in this generic case.

Metal Valence Electron Count	Axial L' Configuration Energy	Equatorial L' Configuration Energy	Preference: Axial or Equatorial L' ?
d^1	$-e_\pi$	$-0.5e_\pi$	Axial
d^2	$-2e_\pi$	$-e_\pi$	Axial
d^3	$-3e_\pi$	$-1.5e_\pi$	Axial
d^4	$-4e_\pi$	$-2e_\pi$	Axial

d^5	$1.125e_\sigma - 4e_\pi$	$1.125e_\sigma - 2.5e_\pi$	Axial
d^6	$2.25e_\sigma - 4e_\pi$	$2.25e_\sigma - 3e_\pi$	Axial
d^7	$3.375e_\sigma - 4e_\pi$	$3.375e_\sigma - 3.5e_\pi$	Axial
d^8	$4.5e_\sigma - 4e_\pi$	$4.5e_\sigma - 4e_\pi$	None
d^9	$7.25e_\sigma - 4e_\pi$	$7.25e_\sigma - 4e_\pi$	None
d^{10}	$10e_\sigma - 4e_\pi$	$10e_\sigma - 4e_\pi$	None

10.15 The angular overlap diagrams for the molecular orbitals with high d orbital character in square pyramidal (left) and trigonal bipyramidal (right) geometries with σ -donor ligands are below. In each of these geometries, the σ -donor ligands pairs are stabilized by $1e_\sigma$; these levels are omitted here.



The energies of the resulting configurations, and the preference between these coordination geometries, depend on electron count and whether the complex is low spin or high spin. The *low spin* configuration energies (ignoring both the exchange energy and the coulombic energy of repulsion contributions) and preferences are:

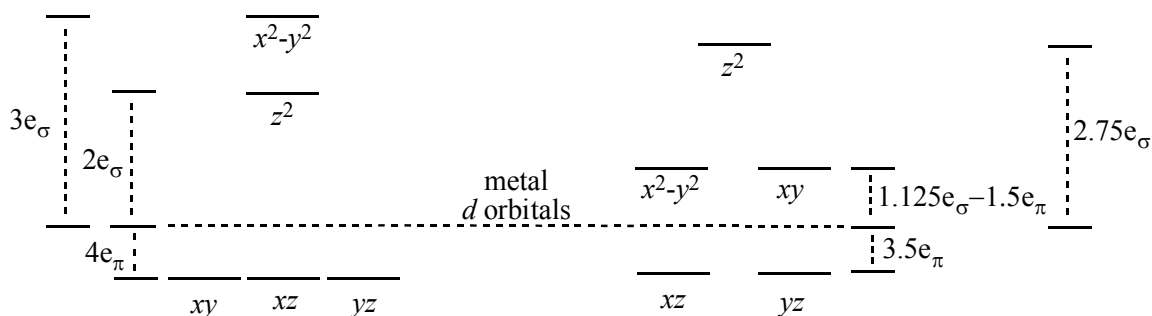
Metal Valence Electron Count	Square Pyramidal Configuration Energy	Trigonal Bipyramidal Configuration Energy	Low Spin Preference
d^1	$0e_\sigma$	$0e_\sigma$	None
d^2	$0e_\sigma$	$0e_\sigma$	None
d^3	$0e_\sigma$	$0e_\sigma$	None
d^4	$0e_\sigma$	$0e_\sigma$	None
d^5	$0e_\sigma$	$1.125e_\sigma$	Square Pyramidal
d^6	$0e_\sigma$	$2.25e_\sigma$	Square Pyramidal
d^7	$2e_\sigma$	$3.375e_\sigma$	Square Pyramidal
d^8	$4e_\sigma$	$4.5e_\sigma$	Square Pyramidal
d^9	$7e_\sigma$	$7.25e_\sigma$	Square Pyramidal
d^{10}	$10e_\sigma$	$10e_\sigma$	None

The corresponding *high spin* preferences (assuming that configurations with five unpaired electrons are lower in energy than five-electron configurations with electron pairs) are:

Metal Valence Electron Count	Square Pyramidal Configuration Energy	Trigonal Bipyramidal Configuration Energy	High Spin Preference
d^1	$0e_\sigma$	$0e_\sigma$	None
d^2	$0e_\sigma$	$0e_\sigma$	None
d^3	$0e_\sigma$	$1.125e_\sigma$	Square pyramidal
d^4	$2e_\sigma$	$2.25e_\sigma$	Square pyramidal
d^5	$5e_\sigma$	$5e_\sigma$	None
d^6	$5e_\sigma$	$5e_\sigma$	None
d^7	$5e_\sigma$	$5e_\sigma$	None
d^8	$5e_\sigma$	$6.125e_\sigma$	Square pyramidal
d^9	$7e_\sigma$	$7.25e_\sigma$	Square Pyramidal
d^{10}	$10e_\sigma$	$10e_\sigma$	None

Although steric configurations are not part of this angular overlap analysis, the trigonal bipyramidal geometry is never preferred relative to square pyramidal in these cases with five σ -donor ligands.

For a set of five σ -donor/ π -acceptor ligands, the energy levels are as follows for square pyramidal (left) and trigonal bipyramidal (right).



The energies of the resulting configurations, and the preference between these coordination geometries, depend on electron count and whether the complex is low spin or high spin. We will assume only *low spin* configurations here since ligands with combined σ -donor/ π -acceptor capabilities tend to stabilize low spin complexes. The *low spin* configuration energies (ignoring both the exchange energy and the coulombic energy of repulsion contributions) and preferences are:

Metal Valence Electron Count	Square Pyramidal Configuration Energy	Trigonal Bipyramidal Configuration Energy	Low Spin Preference
d^1	$-4e_\pi$	$-3.5e_\pi$	Square Pyramidal
d^2	$-8e_\pi$	$-7e_\pi$	Square Pyramidal
d^3	$-12e_\pi$	$-10.5e_\pi$	Square Pyramidal
d^4	$-16e_\pi$	$-14e_\pi$	Square Pyramidal
d^5	$-20e_\pi$	$1.125e_\sigma - 15.5e_\pi$	Square Pyramidal
d^6	$-24e_\pi$	$2.25e_\sigma - 17e_\pi$	Square Pyramidal
d^7	$2e_\sigma - 24e_\pi$	$3.375e_\sigma - 18.5e_\pi$	Square Pyramidal
d^8	$4e_\sigma - 24e_\pi$	$4.5e_\sigma - 20e_\pi$	TBP > SP by only $0.5e_\sigma + 4e_\pi$
d^9	$7e_\sigma - 24e_\pi$	$7.25e_\sigma - 20e_\pi$	Square Pyramidal
d^{10}	$10e_\sigma - 24e_\pi$	$10e_\sigma - 20e_\pi$	Square Pyramidal

Although steric configurations are not part of this analysis, the square pyramidal geometry is clearly preferred relative to trigonal pyramidal in all these cases with five σ -donor/ π -acceptor ligands, except with a d^8 metal where the preference is slight.

10.16 a. Seesaw, using positions 1, 6, 11, and 12 (σ donor only)

Position	z^2	$x^2 - y^2$	xy	xz	yz
1	1	0	0	0	0
6	1	0	0	0	0
11	1/4	3/16	9/16	0	0
12	1/4	3/16	9/16	0	0
Total	2.5	0.375	1.125	0	0

Trigonal pyramidal, using positions 1, 2, 11, and 12 (σ donor only)

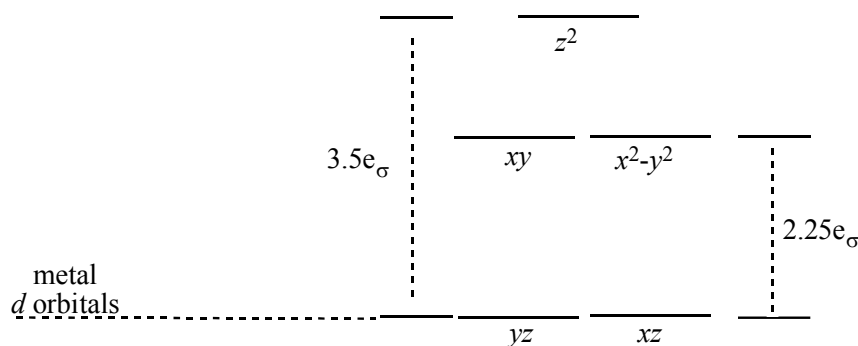
Position	z^2	$x^2 - y^2$	xy	xz	yz
1	1	0	0	0	0
2	1/4	3/4	0	0	0
11	1/4	3/16	9/16	0	0
12	1/4	3/16	9/16	0	0
Total	1.75	1.125	1.125	0	0

b.

Number of <i>d</i> Electrons	Energies of <i>d</i> Configurations (in units of e_{σ})			
	Seesaw		Trigonal Pyramidal	
	Low Spin	High Spin	Low Spin	High Spin
1	0	0	0	0
2	0	0	0	0
3	0	0.375	0	1.125
4	0	1.5	0	2.25
5	0.375	4	1.125	4
6	0.750	4	2.25	4
7	1.875	4	3.375	4
8	3	4.375	4.5	5.125
9	5.5	5.5	6.25	6.25
10	8	8	8	8

c. The seesaw geometry is favored for d^5 — d^9 low spin and d^3 , d^4 , d^8 , and d^9 high spin configurations. For other configurations, both geometries have identical energies according to this approach. (The values shown are for the *d* orbitals only; each interaction also stabilizes a ligand orbital by e_{σ} .)

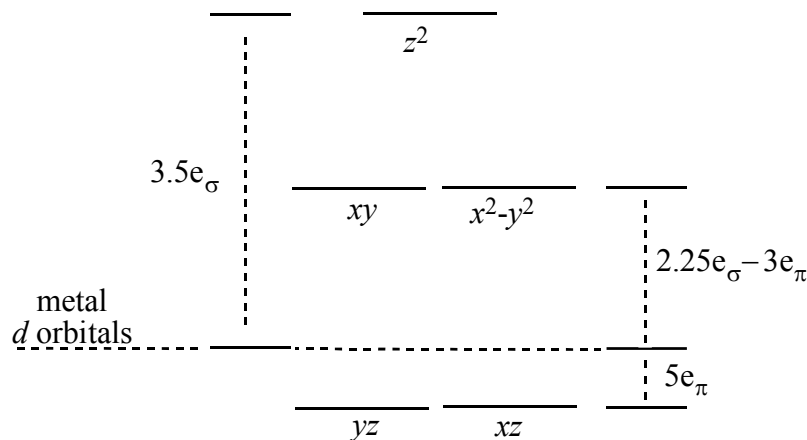
10.17 a. The energies of the molecular orbitals with high *d* orbital character are as follows:



The new positions (13 and 14 below) are opposite 11 and 12, and have the same values in the table. z^2 is affected most strongly, since two ligands are along the z axis; $x^2 - y^2$ and xy are also strongly influenced, since they are in the plane of the six ligands. xz and yz are not changed, since they miss the ligands in all directions.

Position	z^2	$x^2 - y^2$	xy	xz	yz
1	1	0	0	0	0
2	1/4	3/4	0	0	0
6	1	0	0	0	0
11	1/4	3/16	9/16	0	0
12	1/4	3/16	9/16	0	0
4	1/4	3/4	0	0	0
13	1/4	3/16	9/16	0	0
14	1/4	3/16	9/16	0	0
Total	3.5	2.25	2.25	0	0

- b. The D_{6h} character table indicates that z^2 has A_{1g} symmetry, $x^2 - y^2$ and xy have E_{2g} symmetry, and xz and yz exhibit E_{1g} symmetry.
- c. The energies of the molecular orbitals with high d orbital character are as follows:



Position	z^2	x^2-y^2	xy	xz	yz
1	0	0	0	1	1
2	0	0	1	1	0
6	0	0	0	1	1
11	0	3/4	1/4	1/4	3/4
12	0	3/4	1/4	1/4	3/4
4	0	0	1	1	0
13	0	3/4	1/4	1/4	3/4
14	0	3/4	1/4	1/4	3/4
Total	0	$3 e_\pi$	$3 e_\pi$	$5 e_\pi$	$5 e_\pi$
Overall	$3.5 e_\sigma$	$2.25 e_\sigma - 3 e_\pi$	$2.25 e_\sigma - 3 e_\pi$	$-5 e_\pi$	$-5 e_\pi$

- d. If we assume that each low spin configuration will have the maximum number of paired electrons, then the configurations with asymmetrically occupied degenerate orbitals are those for d^1 , d^3 , d^5 , and d^7 metals. These are expected to give rise to Jahn-Teller distortion.

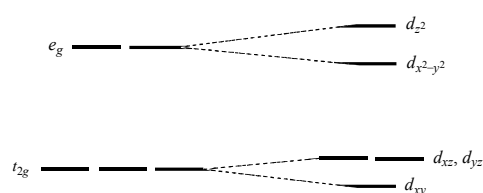
10.18 The ammine Co(III) complex is considerably more stable and is less easily reduced, with the difference primarily in the 3+ species. In addition, the metal in $[\text{Co}(\text{NH}_3)_6]^{3+}$ is surrounded by ammonia molecules, which are more difficult to oxidize than water. This makes transfer of electrons through the ligand more difficult for the ammine complexes.

		LFSE	Δ_o	LFSE	Difference
$[\text{Co}(\text{H}_2\text{O})_6]^{3+}$	d^6 (1s)	$-2.4\Delta_o$	16,750	-40,200	33,480
$[\text{Co}(\text{H}_2\text{O})_6]^{2+}$	d^7 (hs)	$-0.8\Delta_o$	8,400	-6,720	
$[\text{Co}(\text{NH}_3)_6]^{3+}$	d^6 (1s)	$-2.4\Delta_o$	24,000	-57,600	49,440
$[\text{Co}(\text{NH}_3)_6]^{2+}$	d^7 (hs)	$-0.8\Delta_o$	10,200	-8,160	

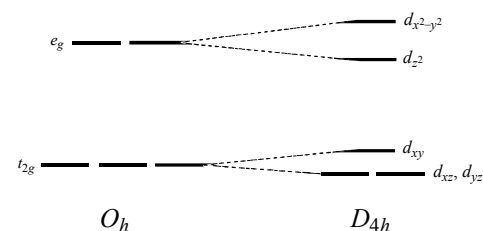
10.19 Cl^- has the lowest Δ_o value and fairly good π donor properties that reduce Δ_o . F^- is next, with less π donor ability. Water has very small π donor ability (only one lone pair not involved in σ bonding), and ammonia and en have nearly insignificant π donor nor acceptor ability (no lone pairs, antibonding orbitals with the wrong shapes and energies for π bonding). CN^- has good π acceptor properties, making Δ_o largest for this ligand.

10.20 Ammonia is a stronger field ligand than water. It is a stronger Lewis base (σ donor) than water. Water also has a lone pair that can act as a π donor (which leads to a reduction in the ligand field splitting). These factors result in the less electronegative nitrogen on ammonia being a better donor atom than the oxygen atom of water. In the halide ions, all have the same valence electronic structure, so the electronegativity is the determining factor in ligand field strength. Fluoride is also a stronger Brønsted base than the other halides.

10.21 a. Compression moves d_{z^2} up in energy and lowers the ligand energies of positions 1 and 6.



b. Stretching reverses the changes. In the limit of a square planar structure, d_{z^2} is affected only through interactions with the ring in the xy plane.



10.22 Cr^{3+} has three singly occupied t_{2g} orbitals and two empty e_g orbitals. As a result, its complexes exhibit no Jahn-Teller distortion. Mn^{3+} has one electron in the e_g orbitals; its complexes show Jahn-Teller distortion.

10.23 a.

	n	μ	LFSE (in Δ_o)
$[\text{Co}(\text{CO})_4]^-$	0	0	0
$[\text{Cr}(\text{CN})_6]^{4-}$	2	2.8	-1.6
$[\text{Fe}(\text{H}_2\text{O})_6]^{3+}$	5	5.9	0
$[\text{Co}(\text{NO}_2)_6]^{4-}$	3	3.9	-0.8
$[\text{Co}(\text{NH}_3)_6]^{3+}$	0	0	-2.4
$[\text{MnO}_4]^-$	0	0	0
$[\text{Cu}(\text{H}_2\text{O})_6]^{2+}$	1	1.7	-0.6

b. The two tetrahedral ions ($[\text{Co}(\text{CO})_4]^-$ and $[\text{MnO}_4]^-$) have zero LFSE (10 or 0 d electrons, respectively) and have ligand equipped to participate in significant π bonding, with CO as an acceptor and O^{2-} as donor. With the exception of $[\text{Fe}(\text{H}_2\text{O})_6]^{3+}$, the others have LFSE values that favor octahedral structures. $[\text{Fe}(\text{H}_2\text{O})_6]^{3+}$ has LFSE = 0 for either

octahedral or tetrahedral shapes, but water is a slight π donor and Fe(III) is only a moderately good π acceptor. As a result, electrostatics favors six ligands.

- c. The difference in the LFSEs can be used to assess the relative stabilities of these geometries for Co(II) and Ni(II):

For Co^{2+} : High-spin octahedral d^7 has $\text{LFSE} = -0.8\Delta_o$
Tetrahedral d^7 has $\text{LFSE} = -1.2\Delta_t = -0.53\Delta_o$

For Ni^{2+} : High-spin octahedral d^8 has $\text{LFSE} = -1.2\Delta_o$
Tetrahedral d^8 has $\text{LFSE} = -0.6\Delta_t = -0.27\Delta_o$

Co(II) (d^7) has only $-0.27\Delta_o$ favoring the octahedral shape, while Ni(II) (d^8) has $-0.93\Delta_o$. Therefore, Co(II) compounds are more likely to be tetrahedral than are Ni(II) compounds.

- 10.24 a.** The ligand field stabilization energies and the $\text{LFSE}_{O_h} - \text{LFSE}_{T_d}$ differences are below. The LFSE is more negative for an octahedral field than the corresponding LFSE for a tetrahedral field, regardless of the ligand field strength. The magnitude of the difference ($\text{LFSE}_{O_h} - \text{LFSE}_{T_d}$) provides some insight into preferences between these geometries for these ions. The likelihood of tetrahedral geometry increases as the energy difference between the octahedral and tetrahedral LFSE decreases. Note that this solution considers both high *and* low spin tetrahedral complexes even though high spin configurations are more common in tetrahedral complexes. The rightmost column provides the difference between the strong field octahedral LFSE and the weak field tetrahedral configurations.

	Octahedral Field LFSE		Tetrahedral Field LFSE		$\text{LFSE}_{O_h} - \text{LFSE}_{T_d}$		
	Weak	Strong	Weak	Strong	Weak — Weak	Strong — Strong	Strong (L.S.) — Weak (H.S.)
$\text{Fe}^{2+} (d^6)$	$-\frac{2}{5}\Delta_o$	$-\frac{12}{5}\Delta_o$	$-\frac{8}{45}\Delta_o$	$-\frac{48}{45}\Delta_o$	$-0.222\Delta_o$	$-1.333\Delta_o$	$-2.22\Delta_o$
$\text{Co}^{2+} (d^7)$	$-\frac{4}{5}\Delta_o$	$-\frac{9}{5}\Delta_o$	$-\frac{16}{45}\Delta_o$	$-\frac{36}{45}\Delta_o$	$-0.444\Delta_o$	$-\Delta_o$	$-1.44\Delta_o$
$\text{Ni}^{2+} (d^8)$	$-\frac{6}{5}\Delta_o$	$-\frac{6}{5}\Delta_o$	$-\frac{24}{45}\Delta_o$	$-\frac{24}{45}\Delta_o$	$-0.667\Delta_o$	$-0.667\Delta_o$	$-0.667\Delta_o$

The magnitudes of the $\text{LFSE}_{O_h} - \text{LFSE}_{T_d}$ differences predict the preference for tetrahedral geometry with weak field ligands to be $\text{Fe}^{2+} > \text{Co}^{2+} > \text{Ni}^{2+}$. The corresponding preference for tetrahedral geometries with a strong field ligand set is predicted as $\text{Ni}^{2+} > \text{Co}^{2+} > \text{Fe}^{2+}$. Note that this ranking is the same with strong field ligands whether the comparison is made to the corresponding high or low spin tetrahedral configuration (the “strong—strong” and “strong—weak” differences offer the same preference rankings). These calculations suggest that the octahedral preference for Fe^{2+} and Co^{2+} is even stronger with a strong field ligand set than with a weak field ligand set.

This approach predicts that the Ni^{2+} preference for octahedral geometry is independent of the ligand field strength.

This LFSE analysis does not match the observation that the number of tetrahedral complexes for these ions ranks as $\text{Co}^{2+} > \text{Fe}^{2+} > \text{Ni}^{2+}$, but does suggest that Co^{2+} is more likely to afford tetrahedral complexes relative to Ni^{2+} when the ligand field is weak.

- b. The energies of these electronic configurations on the basis of the angular overlap model are below. Note that this solution also considers both high *and* low spin tetrahedral complexes even though high spin configurations are more common in tetrahedral complexes. The rightmost column provides the difference between the strong field octahedral and the weak field tetrahedral electronic configurations, respectively. As in **a**, the electronic stabilization afforded by the octahedral field is greater than that provided by a tetrahedral field, with the preference for an octahedral geometry over tetrahedral geometry generally more pronounced with strong field ligands (with Ni^{2+} being an exception with preferences for octahedral geometry that are independent of the ligand field strength).

	Octahedral		Tetrahedral		$O_h - T_d$		
	Weak	Strong	Weak	Strong	Weak	Strong	Strong (L.S.) —Weak (H.S.)
$\text{Fe}^{2+} (d^6)$	$-6e_\sigma$	$-12e_\sigma$	$-4e_\sigma$	$-5.33e_\sigma$	$-2e_\sigma$	$-6.67e_\sigma$	$-8e_\sigma$
$\text{Co}^{2+} (d^7)$	$-6e_\sigma$	$-9e_\sigma$	$-4e_\sigma$	$-4e_\sigma$	$-2e_\sigma$	$-5e_\sigma$	$-5e_\sigma$
$\text{Ni}^{2+} (d^8)$	$-6e_\sigma$	$-6e_\sigma$	$-2.67e_\sigma$	$-2.67e_\sigma$	$-3.33e_\sigma$	$-3.33e_\sigma$	$-3.33e_\sigma$

The magnitudes of the $O_h - T_d$ angular overlap differences predict the preference for tetrahedral geometry with weak field ligands to be $\text{Co}^{2+} \sim \text{Fe}^{2+} > \text{Ni}^{2+}$. The corresponding preference for tetrahedral geometries with a strong field ligand set is predicted as $\text{Ni}^{2+} > \text{Co}^{2+} > \text{Fe}^{2+}$ regardless of whether low spin/low-spin (strong—strong) or low-spin/high spin (strong—weak) configurations are compared.

This angular overlap analysis does not match the observation that the number of tetrahedral complexes for these ions ranks as $\text{Co}^{2+} > \text{Fe}^{2+} > \text{Ni}^{2+}$, but does suggest that the tetrahedral preference is $\text{Co}^{2+} \sim \text{Fe}^{2+} > \text{Ni}^{2+}$ when the ligands are weak. Neither of these approaches is highly predictive in these cases. The complexity of the effects that govern geometric preferences cannot be encompassed in any single approach.

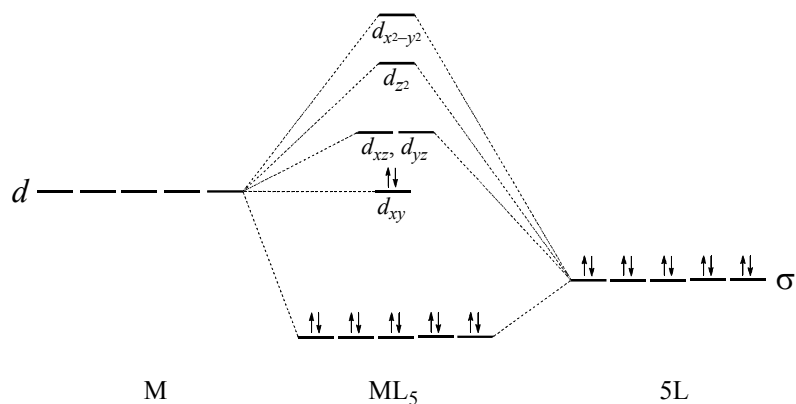
- 10.25** The energy levels of the square planar d orbitals are shown in Figure 10.14; those of the octahedral orbitals are shown in Figure 10.5. The seventh, eighth, and ninth d electrons in an octahedral complex go into the highest orbitals, raising the total energy of the complex. In a square planar complex, the seventh and eighth metal d electrons occupy a relatively nonbonding orbital. When strong field π -acceptor ligands are employed, the Δ_o between the t_{2g} and e_g orbitals increases in octahedral complexes, further stabilizing configurations with 6 or less metal

d electrons. In these cases, the energy of the square planar complex may be more favorable even though the total ligand electron energy is less than in octahedral complexes because there are only four ligands rather than six.

10.26 a. Square pyramidal complexes have C_{4v} symmetry.

C_{4v}	E	$2C_4$	C_2	$2\sigma_v$	$2\sigma_d$	
Γ	5	1	1	3	1	
A_1	1	1	1	1	1	z, z^2
B_1	1	-1	1	1	-1	$x^2 - y^2$
E	2	0	-2	0	0	$(x, y), (xz, yz)$

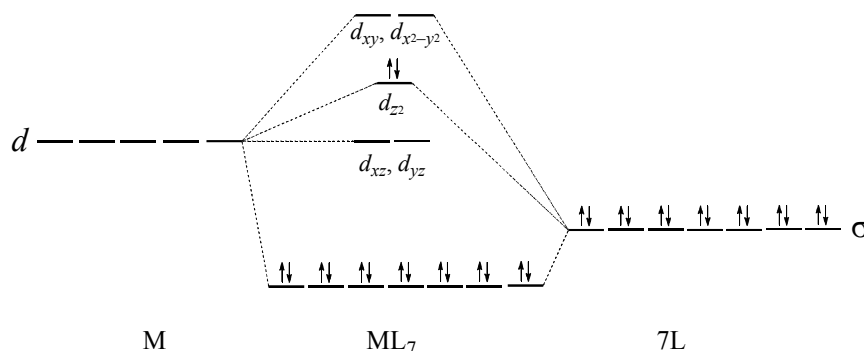
The z^2 and $x^2 - y^2$ orbitals are the major d orbitals used in the bonding, so the d orbital energies are as shown at right. The z^2 orbital is less involved because it is directed primarily toward one ligand, and the $x^2 - y^2$ orbital is directed toward four ligands.



b. Pentagonal bipyramidal complexes have D_{5h} symmetry.

D_{5h}	E	$2C_5$	$2C_5^2$	$5C_2$	σ_h	$2S_5$	$2S_5^3$	$5\sigma_v$	
Γ	7	2	2	1	5	0	0	3	
A_1'	1	1	1	1	1	1	1	1	z^2
E_1'	2	$2 \cos 72^\circ$	$2 \cos 144^\circ$	0	2	$2 \cos 144^\circ$	$2 \cos 72^\circ$	0	(x, y)
E_2'	2	$2 \cos 144^\circ$	$2 \cos 72^\circ$	0	2	$2 \cos 72^\circ$	$2 \cos 144^\circ$	0	$(x^2 - y^2, xy)$
A_2''	1	1	1	-1	-1	-1	-1	1	z

The representation Γ reduces to $2A_1' + E_1' + E_2' + A_2''$. The d orbitals are in three sets, including a nonbonding pair (d_{xz} and d_{yz}) in addition to the A_1' and degenerate E_2' .



10.27 The angular overlap parameters are (Cl), 5430 cm^{-1} ; $e_{\pi}(\text{Cl})$, 1380 cm^{-1} ;

$e_{\sigma}(\text{PPh}_3)$, 3340 cm^{-1} ; $e_{\pi}(\text{PPh}_3)$, -310 cm^{-1} . Application of these values using Tables 10.10 and 10.11 with the ligand positions arbitrarily defined as shown, provides these results:

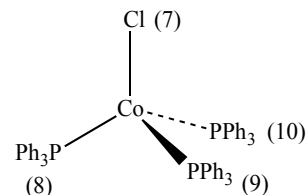
Stabilization of Donor Pairs

$$(7) \quad 1e_{\sigma}(\text{Cl}) + 2e_{\pi}(\text{Cl}) = 8190 \text{ cm}^{-1}$$

$$(8) \quad 1e_{\sigma}(\text{PPh}_3) = 3340 \text{ cm}^{-1}$$

$$(9) \quad 1e_{\sigma}(\text{PPh}_3) = 3340 \text{ cm}^{-1}$$

$$(10) \quad 1e_{\sigma}(\text{PPh}_3) = 3340 \text{ cm}^{-1}$$



The three π acceptor orbitals associated with the PPh_3 ligands are *destabilized* by

$$\frac{2}{3}e_{\pi}(\text{PPh}_3) = 207 \text{ cm}^{-1}.$$

The energies of the molecular orbitals with high metal d orbital character are shown below. The triphenylphosphine and chloride σ interactions and the chloride π interactions contribute to the destabilization of these orbitals, while the π -acceptor capability of triphenylphosphine slightly lowers the energies of the xy , xz , and yz orbitals.

$$z^2 \quad \frac{2}{3}e_{\pi}(\text{Cl}) + 2e_{\pi}(\text{PPh}_3) = 300 \text{ cm}^{-1}$$

$$x^2 - y^2 \quad \frac{2}{3}e_{\pi}(\text{Cl}) + 2e_{\pi}(\text{PPh}_3) = 300 \text{ cm}^{-1}$$

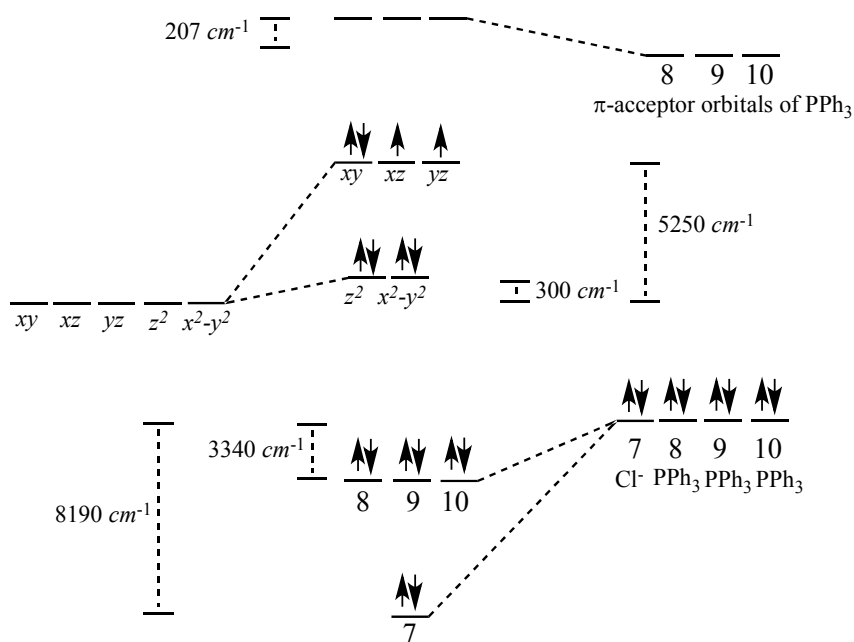
$$xy \quad 1e_{\sigma}(\text{PPh}_3) + \frac{1}{3}e_{\sigma}(\text{Cl}) + \frac{2}{9}e_{\pi}(\text{Cl}) + \frac{2}{3}e_{\pi}(\text{PPh}_3) = 5250 \text{ cm}^{-1}$$

$$xz \quad 1e_{\sigma}(\text{PPh}_3) + \frac{1}{3}e_{\sigma}(\text{Cl}) + \frac{2}{9}e_{\pi}(\text{Cl}) + \frac{2}{3}e_{\pi}(\text{PPh}_3) = 5250 \text{ cm}^{-1}$$

$$yz \quad 1e_{\sigma}(\text{PPh}_3) + \frac{1}{3}e_{\sigma}(\text{Cl}) + \frac{2}{9}e_{\pi}(\text{Cl}) + \frac{2}{3}e_{\pi}(\text{PPh}_3) = 5250 \text{ cm}^{-1}$$

(Continued)

The energy level diagram is:



The large degree of stabilization of the chloride donor pair relative to the PPh_3 pairs is surprising; triphenylphosphine is generally considered a stronger field ligand relative to chloride. The steric bulk associated with the coordination of three PPh_3 ligands to the Co(I) center may attenuate the donor ability (and acceptor ability) of these ligands in $\text{CoCl(PPh}_3)_3$. The increased σ -donation of PPh_3 and increased π -donation of Cl in $\text{NiCl}_2(\text{PPh}_3)_2$ relative to $\text{CoCl(PPh}_3)_3$, respectively, is likely linked to the higher oxidation state of Ni(II) relative to the Co(I) . The reduced steric bulk about the Ni(II) center in $\text{NiCl}_2(\text{PPh}_3)_2$ relative to around the Co(I) center in $\text{CoCl(PPh}_3)_3$ likely plays a role in increasing the overlap necessary for the π -interactions.

- 10.28 a.** The MO diagram is similar to that for CO , shown in Figure 5.13, with the atomic orbitals of fluorine significantly lower than the matching orbitals of nitrogen. The NF molecule has 2 more electrons than CO ; these occupy π^* orbitals and have parallel spins.
- b.** Because its highest occupied sigma orbital (labeled $5a_1$ for CO) is significantly concentrated on the nitrogen, NF should act as a strong σ donor. In addition, because the π^* orbitals are also strongly concentrated on nitrogen, NF should act as a π acceptor at nitrogen. Because the π^* orbitals are singly occupied, NF is likely to be a weaker π acceptor than CO , whose π^* orbitals are empty. Overall, NF is likely to be relatively high in the spectrochemical series, but lower than CO .
- 10.29 a.** When these compounds are oxidized, in the positively charged products there is less π acceptance by the CO ligands than in the neutral compounds. Because CO is acting less as a π acceptor in the products, the products have less donation into their π^* orbitals, which are antibonding with respect to the C-O bonds. This means that the oxidation products have stronger and shorter C-O bonds than the reactants. In the reference cited, the C-O bonds are calculated to be shortened by 0.014 to 0.018 Å in the PH_3 complex and by 0.015 to 0.020 Å in the NH_3 complex.

- b. In the phosphine compound, oxidation reduces the π acceptance by the phosphine (as it reduces the π acceptance by the carbonyls), and there is weaker Cr–P bonding. Therefore, the Cr–P bond is longer in the product (by 0.094 Å).

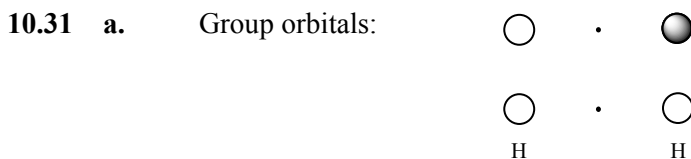
In the ammine compound, the NH_3 is not a π acceptor; it is a σ donor only. Because oxidation increases the positive charge on the metal, there is stronger attraction between the metal and the sigma-donating NH_3 , shortening the Cr–N bond (by 0.050 Å).

10.30 The structure of $[\text{ReH}_9]^{2-}$ (Figure 9.35) has a D_{3h} point group.

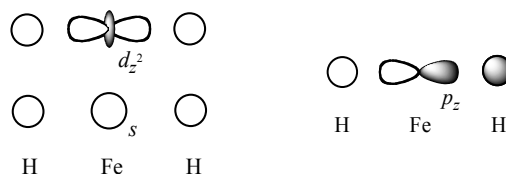
D_{3h}	E	$2C_3$	$3C_2$	σ_h	$2S_3$	$3\sigma_v$	
Γ	9	0	1	3	0	3	
A_1'	1	1	1	1	1	1	$x^2 + y^2, z^2$
E'	2	-1	0	2	-1	0	$(x, y) (x^2 - y^2, xy)$
A_2''	1	1	-1	-1	-1	1	z
E''	2	-1	0	-2	1	0	(xz, yz)

The representation Γ reduces to $2A_1' + 2E' + A_2'' + E''$. These representations match atomic orbitals on Re as follows:

$$\begin{array}{ll}
 A_1' & s, d_{z^2} \\
 E' & (p_x, p_y), (d_{x^2-y^2}, d_{xy}) \\
 A_2'' & p_z \\
 E'' & (d_{xz}, d_{yz})
 \end{array}$$



- b. Group orbital–central atom interactions:



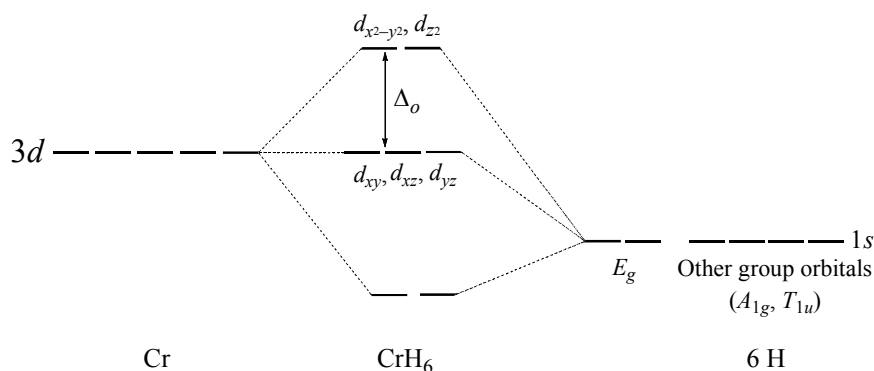
- c. The hydrogen orbitals (potential energy = -13.6 eV) are likely to interact more strongly with iron orbitals that have a better energy match, the $3d$ (-11.7 eV) and $4s$ (-7.9 eV). The $3p$ orbitals of iron are likely to have very low energy (ca. -30 eV) and not to interact significantly with the hydrogen orbitals. (Potential energies for transition metal orbitals can be found in J. B. Mann, T. L. Meek, E. T. Knight, J. F. Capitani, and L. C. Allen, *J. Am. Chem. Soc.*, **2000**, *122*, 5132.)

10.32 a. In octahedral geometry the s orbitals on the hydride ligands would generate the representation:

O_h	E	$8C_3$	$6C_2$	$6C_4$	$3C_2(=C_4^2)$	i	$6S_4$	$8S_6$	$3\sigma_h$	$6\sigma_d$	
Γ	6	0	0	2	2	0	0	0	4	2	
A_{1g}	1	1	1	1	1	1	1	1	1	1	
E_g	2	-1	0	0	2	2	0	-1	2	0	$(2z^2-x^2-y^2, x^2-y^2)$
T_{1u}	3	0	-1	1	-1	-3	-1	0	1	1	(x, y, z)

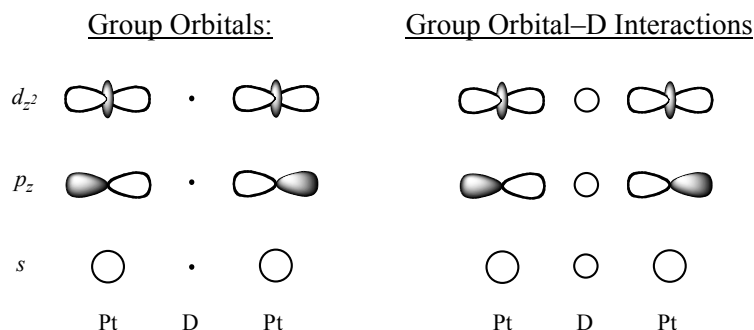
b. The representation reduces to $A_{1g} + E_g + T_{1u}$, as shown above.

c. The matching orbitals on Cr are: A_{1g} : s ; E_g : $d_{x^2-y^2}, d_{z^2}$; T_{1u} : p_x, p_y, p_z . The orbital potential energies for the Cr $3d$ orbitals and H $1s$ orbitals are -10.75 eV and -13.61 eV, respectively. The energy compatibility of these orbitals suggests the possibility of a relatively robust interaction between the Cr $d_{x^2-y^2}, d_{z^2}$ orbitals and the group orbitals comprised of hydrogen $1s$ orbitals.



10.33 a. D_{4h}

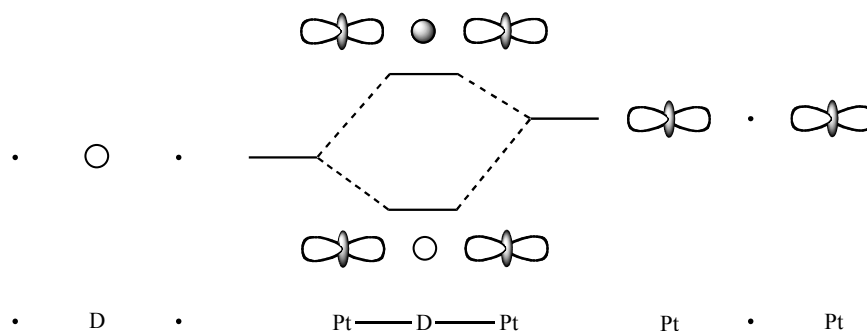
b. 1. Because a deuterium atom has only its $1s$ electron to participate in bonding, there are only three platinum group orbitals that can potentially interact with deuterium:



2. In each case, sigma interactions could occur, as shown above.

3. The strongest interactions are most likely between the d_{z^2} orbitals of Pt and the $1s$ orbital of D. Lobes of the $5d_{z^2}$ orbitals point toward the D, and their energy (-10.37 eV) is a good match for the valence orbital potential energy of hydrogen

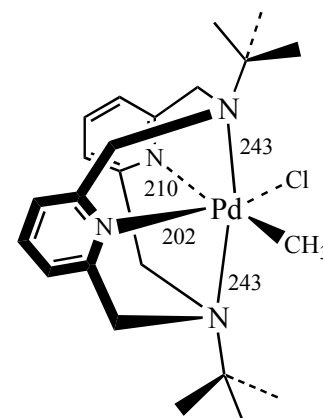
(−13.61 eV). Both bonding and antibonding molecular orbitals would be formed:



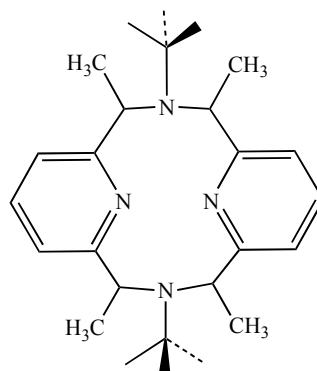
10.34 MnO_4^- has no d electrons, while MnO_4^{2-} has 1. The slight antibonding effect of this electron is enough to lengthen the bonds. In addition, there is less electrostatic attraction by Mn(VI) in MnO_4^{2-} than by Mn(VII) in MnO_4^- .

10.35 The oxidation product is sketched at right, with the Pd—N distances (pm) provided. The longer Pd—N axial distances (243 pm) relative to the equatorial Pd—N distances (202 and 210 pm) illustrate the Jahn-Teller distortion. The reference indicates that the HOMO has extensive character of the Pd $4d_{z^2}$ orbital. This orbital also features significant sp^3 character at the axial nitrogen atoms.

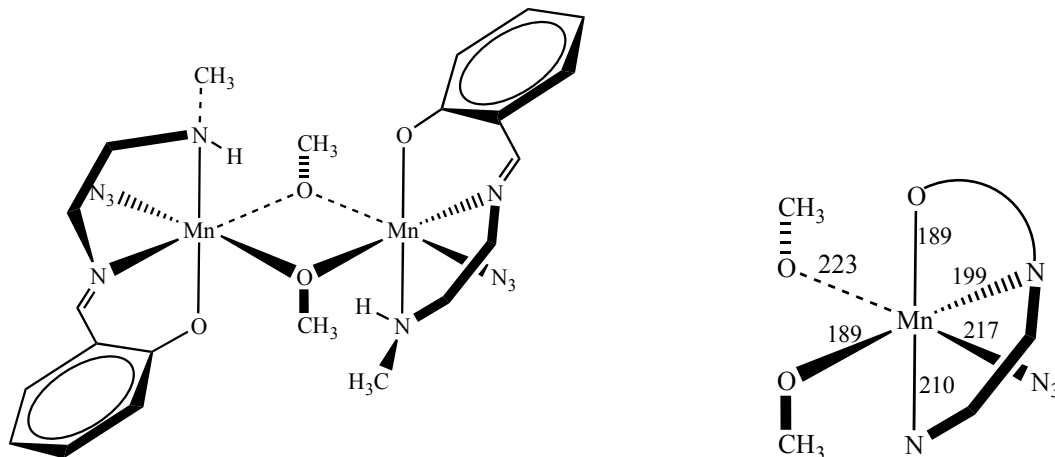
Using a ligand with more electron-rich axial nitrogen atoms could possibly increase the energy of the HOMO. One proposal would be the introduction of electron-releasing methyl substituents at the (now) methylene carbons α the tertiary amine nitrogen atoms. One ligand candidate is below.



One challenge in “ligand design” is that modifications of a molecule will sometimes prevent its subsequent metal binding (for example, if steric bulk near the donor atoms increases too much). And the synthesis of new ligands often presents significant research challenges, even when the desired modification appears minor.

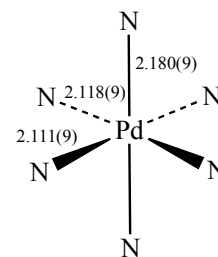


- 10.36** The dimeric structure of $[\text{Mn}^{\text{I}}(\text{N}_3)(\text{OCH}_3)]_2$ is below, with an abbreviated sketch of the Mn(III) coordinate sphere with bond lengths (pm) at right. The reference states that the three donor atoms of the meridionally coordinated Schiff base ligand and the bridging oxygen atom 189 pm from Mn(III) form an equatorial plane in this distorted octahedral geometry. The significantly longer bond length to the other bridging oxygen atom (223 pm) suggests the presence of Jahn-Teller distortion, but the possibility of a *trans* effect of the azide ligand (Section 12.7) must also be considered.



- 10.37.** The structure of $[\text{Pd}(\text{tacn})(\text{Htacn})]^{3+}$ is surprising since both non-coordinated nitrogen atoms are positioned on the same side of the plane formed by the four nitrogen atoms bound to the Pd(II) center (*syn*). This creates more steric hindrance than would be provided by an *anti* structure. The authors suggest that the orientation of these nitrogen atoms maximizes hydrogen bonding with the nitrate counterions and water in the solid state. An alternate explanation not explicitly stated is an intramolecular hydrogen bond involving both N(1) and N(1)′.

The palladium-nitrogen core of $[\text{Pd}(\text{tacn})_2]^{3+}$ is sketched at right (bond lengths in Å with estimated standard deviations), with the slight elongation in the Pd—N(axial) bonds indicating Jahn-Teller distortion. The three unlabeled bonds are equivalent to those *trans* to them by symmetry; they have the identical bond distances.



- 10.38 a.**

O_h	E	$8C_3$	$6C_2$	$6S_4$	$3C_2(=C_4^2)$	i	$6S_4$	$8S_6$	$3\sigma_h$	$6\sigma_d$	
Γ	6	0	0	2	2	0	0	0	4	2	
A_{1g}	1	1	1	1	1	1	1	1	1	1	
E_g	2	-1	0	0	2	2	0	-1	2	0	$(2z^2 - x^2 - y^2, x^2 - y^2)$
T_{1u}	3	0	-1	1	-1	-3	-1	0	1	1	(x, y, z)

- b.** The representation reduces to $A_{1g} + E_g + T_{1u}$, as shown above.
- c.** The matching orbitals on Ti are: A_{1g} : s ; E_g : $d_{x^2-y^2}, d_{z^2}$; T_{1u} : p_x, p_y, p_z

